

Polaronic hole-trapping in doped BaBiO₃

C. Franchini,¹ G. Kresse,¹ and R. Podloucky²

¹ Faculty of Physics, Universität Wien and Center for Computational Materials Science, A-1090 Wien, Austria

² Institute for Physical Chemistry and Center for Computational Materials Science, Vienna University, Sensengasse 8, A-1090 Vienna, Austria

(Dated: May 13, 2009)

The present *ab initio* study shows that in BaBiO₃, Bi³⁺ sites can trap two holes from the valence band to form Bi⁵⁺ cations. The trapping is accompanied by large local lattice distortions, therefore the composite particle consisting of the electronic-hole and the local lattice phonon field forms a polaron. Our study clearly shows that even *sp* elements can trap carriers at lattice sites, if local lattice relaxations are sufficiently large to screen the localised hole. The derived model describes all relevant experimental results, and settles the issue of why hole doped BaBiO₃ remains semiconducting upon moderate hole doping.

PACS numbers: 71.30.+h, 71.38.-k, 71.45.Lr, 78.20.-e

The nature of insulator-metal(superconductor) transitions in oxides has intrigued scientists for several decades[1, 2, 3]. Such transitions can be realised by modulating the electrical carrier density using electric field effects, chemical doping or pressure[4, 5]. Despite the intense experimental and theoretical efforts, an atomistic interpretation of the experimental data is often exceedingly difficult, since the available first principles methods are too approximate. BaBiO₃ is a prime example for such a phenomenon because it is a charge-ordered insulator, in which bismuth atoms appear in two different oxidation states (3+ and 5+). It undergoes an insulator-superconductor transition upon hole doping[6]. Here we demonstrate that up to 0.25 holes per formula unit, the charge-ordered insulating state prevails, but an insulator to metal transition is predicted beyond a hole concentration of about 0.3 holes per formula unit. We show that the transition is controlled by the coupling between the

additional holes trapping on original Bi³⁺ sites and the oxygen polarisation fields that surround the BiO₆ octahedra. The composite particle, composed of a hole plus its accompanying polarisation field (distortion) is known as a polaron[7]

The primitive cell of BaBiO₃ can be described as Ba₂²⁺Bi³⁺Bi⁵⁺O₆²⁻, where Bi⁵⁺ and Bi³⁺ cations occur in equal parts[8, 9]. Indeed, the two different valencies of bismuth are manifested in the measured structural properties, from which two different bismuth-oxygen bond lengths are derived: the shorter bond length is attributed to Bi⁵⁺-O bonds, the larger one to Bi³⁺-O bonds[8]. At low temperatures, the two Bi species are alternatingly ordered in a distorted cubic (monoclinic) structure, in which Bi⁵⁺ is surrounded by Bi³⁺ neighbours (and vice versa), as sketched in Fig. 1(a) and (b). Upon K doping, Ba_{1-x}K_xBiO₃ undergoes a phase transition to an orthorhombic, still perovskite like semiconducting phase, at a composition of $x \approx 0.12$ [10]. Finally for larger K concentrations $0.37 < x < 0.53$, the compound becomes superconducting[6] with no measurable distortions. *Ab initio* modelling for such a case is problematic, since standard semi-local exchange-correlation functionals, such as the local density approximation or the generalised gradient approximation, predict a too small charge disproportionation describing BaBiO₃ as a metal[11, 12, 13], in disagreement with the experimental observations[14]. Since already the parent material is described incorrectly by semi-local functionals, density functional theory (DFT) calculations for hole doped BaBiO₃ are unreliable, and until today an atomistic understanding of why BaBiO₃ remains semiconducting upon replacing the divalent Ba by monovalent K is missing.

The drawbacks of semi-local density functionals are mainly related to sizeable self-interactions[15, 16]. A theory that is largely self-interaction free is therefore a prerequisite to model BaBiO₃, and for this, hybrid functionals mixing a fraction of non-local Hartree-Fock exchange (typically 25 %) to the otherwise semi-local exchange are

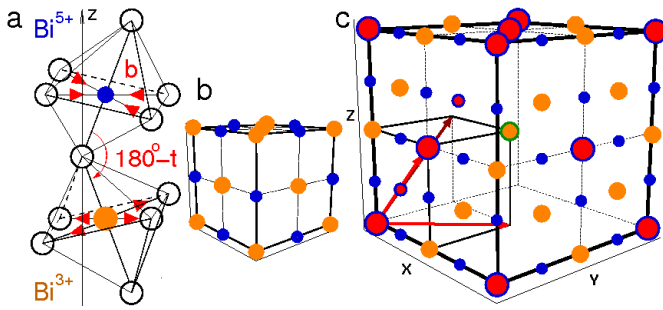


FIG. 1: (a) Monoclinically distorted BiO₆ octahedra emphasising the tilting (*t*) and breathing (*b*) structural instabilities around inequivalent Bi³⁺ (orange) and Bi⁵⁺ (blue) atoms. (b) Sketch of the simple cubic (sc) small superlattice comprising 8 BiO₆ octahedra. (c) Representation of the large face centred cubic (fcc) supercell (16 BiO₆ octahedra) adopted to model the polaronic states for $x = 0.125$ and 0.25 , with red arrows indicating the Bravais lattice vectors. Red atoms indicate Bi³⁺ ions converted into Bi⁵⁺ ions upon hole-doping for $x = 0.125$ (large balls) and $x = 0.25$ (large and small balls).

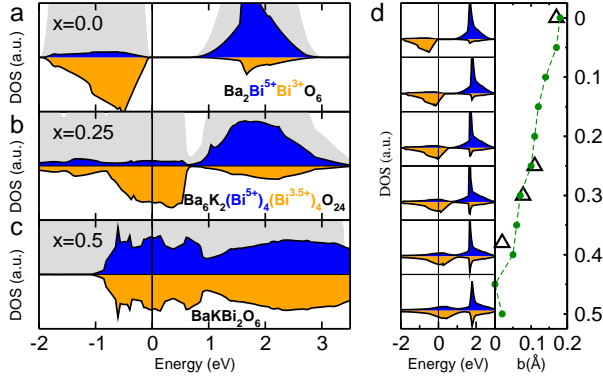


FIG. 2: (Colour online) (a-c) Evolution of the density of states (DOS) on Bi^{3+} (orange) and Bi^{5+} (blue) atoms with K hole doping x for the non-polaronic solution (superlattice with 8 unit cells). The gray shadows indicate the total DOS. (d) Evolution of the DOS of hole-doped BaBiO_3 simulated by removing a fraction of an electron (x) leading to a reduction of the gap between the Bi^{3+} and Bi^{5+} sub-bands, and the simultaneous reduction of the Bi-O bond length difference b between Bi^{3+} and Bi^{5+} sites. Symbols Δ represent the estimated values of the breathing distortion b computed from the Rice and Wang gap equation[22].

a promising choice[17]. In the present work, all calculations are based on the Heyd-Scuseria-Ernzerhof (HSE) hybrid functional[18] and were carried out using the Vienna *ab-initio* simulation package (VASP)[19, 20]. This functional can be applied to metallic systems, since the long range tail of the Coulomb kernel is screened.

For pure BaBiO_3 , HSE correctly predicts a semiconducting state with an indirect band gap of 0.65 eV [see Fig. 2(a)], exhibiting Bi^{3+} and Bi^{5+} sites. For these two sites, the Bi-O bond lengths differ by $b=0.18$ Å, which is in excellent agreement with experiment ($b=0.17$ Å)[8]. The calculated tilting instability $t=11.9^\circ$ correlates also very well with the measured value of 11.2° [8]. The density of states shown in Fig. 2(a) clearly shows that the valence band is dominated by orbitals located predominantly on Bi^{3+} atoms and the surrounding oxygen atoms, whereas the conduction band is dominated by orbitals located close to the Bi^{5+} atoms. It should be noted that we keep the simple formal notation of 3+ and 5+ for the Bi-ions, although the actual charge transfer is reduced by screening, hybridisation and back-donation as a result of the selfconsistent treatment. We will first concentrate on the hole doped system without polaronic distortion, and then discuss how polaronic distortions modify the electronic and lattice structure.

The non-polaronic state was modelled using a supercell comprising 8 perovskite unit cells [Fig. 1(b)]. For the initial structures— before relaxing the structural parameters—the BiO_6 octahedra were tilted in accordance to the monoclinic structure of Fig. 1(a). In this supercell, we replaced 2 or 4 of the original 8 Ba atoms by K atoms,

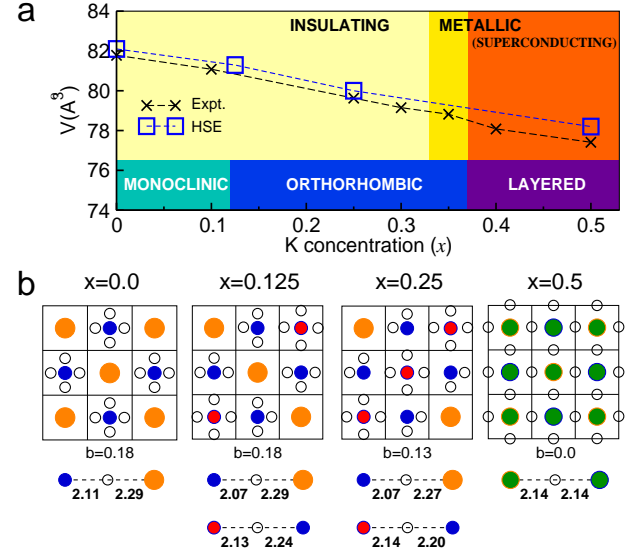


FIG. 3: (a) Phase diagram and volume (V) of $\text{Ba}_{1-x}\text{K}_x\text{BiO}_3$ upon doping throughout the insulator-metal transition. The computed volumes are compared to neutron powder diffraction data[10]. (b) Schematic structure of the Bi-O plane for the insulating charge ordered state of pure BaBiO_3 ($x = 0$), the bipolaronic phases at $x = 0.125$ and $x = 0.25$ and the metallic regime at $x = 0.5$, showing the local oxygen (\circ) breathing environment around Bi^{3+} (\bullet), Bi^{5+} (\bullet), bipolaron $\text{Bi}^{3+} \rightarrow \text{Bi}^{5+}$ (\bullet), and $\text{Bi}^{4.5+}$ (\bullet) sites. Bi-O bond lengths between different sites are displayed.

corresponding to a hole doping concentration of $x = 0.25$ and $x = 0.5$, respectively.

For $x = 0.25$, the calculations predict that the two substitutional K atoms prefer to be arranged along the [001] direction resulting in an orthorhombic supercell after relaxation. The predicted lattice parameters agree well with the experimentally observed orthorhombic structure at $x = 0.25$ (theory: $a = 6.11$ Å, $b = 6.087$ Å, $c = 8.606$ Å; experiment[10]: $a = 6.098$ Å, $b = 6.086$ Å, $c = 8.584$ Å). For $x = 0.5$, K layers parallel to the (100) planes are preferred. The final relaxed structure is non-centrosymmetric and tetragonal, and the structural parameters again agree very well with the experimental values (theory: $a = b = 4.27$, $c/a = 2.01$, experiment[21]: $a = b \approx 4.26$, $c/a \approx 2.0$).

The density of states shown in Fig. 2(b) shows that the Fermi-level moves into the Bi^{3+} dominated valence band, and therefore the system becomes metallic. Furthermore, as a result of the reduced charge disproportionation, the Bi^{3+} states move upwards in energy until the valence and conduction bands overlap [Fig. 2(c)]. At $x = 0.5$ charge disproportionation is no longer sustained 2(c). We also simulated this effect by electronic hole doping in the primitive cell ($\text{Ba}_2\text{Bi}_2\text{O}_6$) finding quantitatively similar results as for K induced hole doping [Fig. 2(d)], indicating that chemical effects do not play a major role.

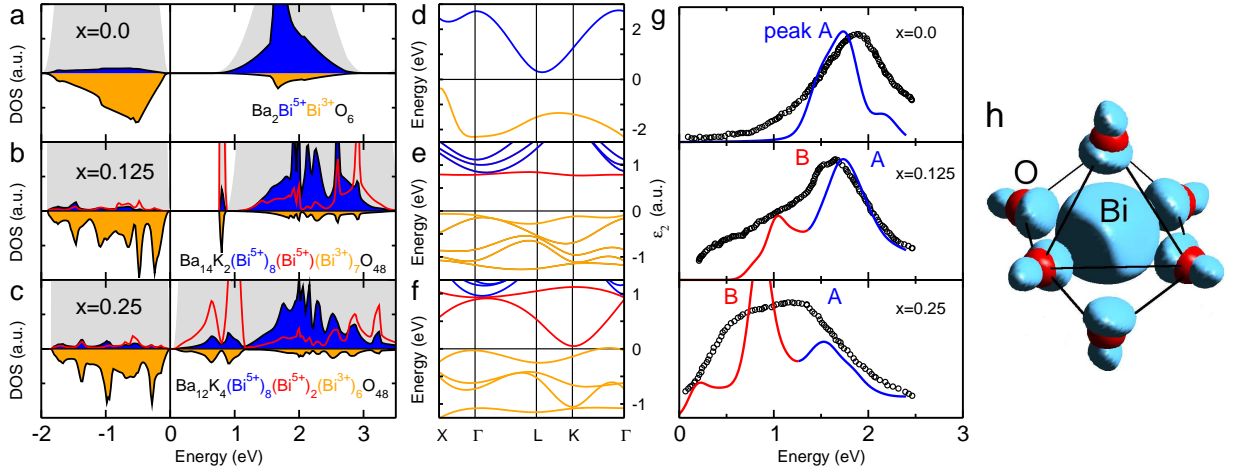


FIG. 4: (a-c) Evolution of the DOS and (d-f) corresponding bandstructure upon K substitution for the polaronic solution. The gray shadows indicate the total density of states, and red curves indicate the bipolaronic states as created by doping. (g) Comparison between the theoretical and measured imaginary part of the dielectric function for $x=0$, 0.125 and 0.25. Peak (A) corresponds to excitations from Bi^{3+} into Bi^{5+} states, peak (B) corresponds to excitations from Bi^{3+} into bipolaronic states [red curves in panel (b),(c),(e), and (f)]. The experimental curves (e) are taken from Ref. 23 ($x=0$) and Ref. 24 ($x=0.21$). For the calculated curves, the excitation energies have been scaled by a factor of 0.8 to approximately account for excitonic effects otherwise not included in the calculations. (h) Charge density corresponding to the bipolaronic band (red line) of panel (e) localised around the BiO_6 octahedron at the converted $\text{Bi}^{3+} \rightarrow \text{Bi}^{5+}$ atom.

Although the above description accounts well for the structural properties and the change in volume [see Fig. 3(a)], the Fermi-level is located in the valence band for any sizable hole concentration, resulting in a strong intra-band metallic behaviour, in contradiction with experiment[23, 24]. On the other hand, polarons allow the stabilisation of an insulating groundstate.

The *isolated polaron* was modelled in an fcc like supercell with 16 BaBiO_3 unit cells [Fig. 1(c)] replacing two Ba atoms by K atoms ($x=0.125$). The BiO_6 octahedra were again initially tilted as in the monoclinic structure. Within this setup the trapping of the two holes on one former Bi^{3+} lattice site emerges naturally during relaxation. Remarkably, hole trapping and local lattice relaxations are strongly linked. Hence we encounter a truly polaronic behaviour. Since a single Bi^{3+} cation captures two holes, we will refer to this Bi lattice site as “bipolaron” from now on[7, 25]. The final relaxed model is clearly insulating [Fig. 4(b)] with an electronic structure that is similar to the one of pure BaBiO_3 . The two holes are confined in one single unoccupied band below the bottom of the conduction band [Fig. 4(e)]. The hole trapping is accompanied by a fairly large local relaxation and since converted sites have only Bi^{5+} neighbours, they are structurally frustrated and do not order within the same local breathing environment as the non-frustrated original Bi^{5+} atoms, as depicted in detail in Fig.3(b).

The spatial charge distribution of the narrow bipolaronic band is shown in Fig. 4(h). Only about 15 % of the charge is localised on the Bi site, the rest is partially located on the surrounding O atoms and a significant

amount of charge is also dispersed throughout the cell (not shown). This distinguishes *sp* systems from *d* or *f* dominated materials. Fig. 4(h) shows that the band is made up by an antibonding linear combination between the Bi *s* orbital and the surrounding O *p* orbitals (nodal planes along Bi-O bonds). Hence the lattice distortion accompanying the bipolaron is driven by moving the antibonding Bi-O state above the Fermi-level. The bonding state is occupied and found in the O subband. This results in the observed contraction of the O-Bi bond length for the converted Bi site (2.13 Å) with respect to the non-converted Bi^{3+} sites (2.29 Å). Attempts to stabilise such a solution using more approximate techniques such as a one-centre LDA+U treatment failed for this material, since the Bi *s* orbitals are too delocalised.

Interaction between polarons: stabilising the polaronic solution at a larger hole concentration ($x=0.25$) turned out to be rather difficult. To minimise bipolaron-bipolaron interactions, one might naively expect the bipolarons to arrange in a $2 \times 2 \times 2$ super-lattice. But relaxation from such a starting structure always turned into a metallic state [see Fig. 1(b)]. In the fcc like supercell with 16 BaBiO_3 unit cells, however, a brief and completely unbiased molecular dynamics run, followed by relaxation yields an insulating state. A string of Bi^{3+} atoms along the face diagonal [101] converts into Bi^{5+} atoms, each trapping two holes [Fig. 1(c)]. Similar bipolaronic alignments along all three face diagonals are found to be energetically almost degenerate, all leading towards a similar insulating state as displayed in Figs. 4(c) and (f). Compared to the metallic state the insulat-

ing solution is about 150 meV/polaron lower in energy. The sc arrangement of bipolarons [Fig. 1(b)] was consistently metallic for symmetry reasons (lack of some Bragg reflections for this arrangement) [26]. As a result of the small distance between the bipolarons, we find a rather strong electronic interaction between them. The bipolaronic subband [Fig. 4(c)] is split into a lower broad band and a relatively narrow second subband [Fig. 4(f)]. The observed band structure is consistent with weakly interacting s like impurity states, with the lower (upper) subband corresponding to bonding (anti-bonding) linear combinations of bipolaronic states. Although the interaction between bipolarons will partially depend on the long range order, the strong interaction beyond $x = 0.125$ might well be the origin of the experimentally observed monoclinic to orthorhombic phase transition at $x \approx 0.12$. The strong interaction ultimately also causes an overlap between the bipolaronic band and the valence band resulting in the metallic non-disproportionated state observed in our calculations at $x = 0.5$ [Fig. 2(c)]. A proper description of the superconducting state emerging at these high doping concentrations will require the inclusion of electron-phonon coupling. For the insulating state, however, we expect only minor modifications due to electron-phonon coupling.

The comparison between the experimental and the calculated imaginary part of the dielectric function (ϵ_2) shown in Fig. 4(g) confirms that our model captures all essential features. In pure BaBiO_3 a single adsorption peak (A) is visible corresponding to the charge-ordered excitation between the Bi^{3+} and Bi^{5+} sub-bands. At $x = 0.125$, a second peak (B) emerges related to the excitation from the valence Bi^{3+} band into the bipolaronic band. It should be noted that disorder and finite temperature effects (electron-phonon interaction) will broaden the theoretical peaks thus improving the agreement with experiment. At $x = 0.25$, the bipolaronic peak (B) increases significantly in intensity and shifts towards lower energy, whereas peak A loses intensity. Considering that our calculations neglect disorder and approximate excitonic effects, our results compare well with experiment and qualitatively explain the emergence of peak B in the experimental spectra, its low intensity at low doping concentrations, the downshift and increase in intensity at larger doping concentrations (bipolaron-bipolaron interaction), as well as the bleaching of the A mode.

In summary, we have shown that sp like electronic holes can trap at otherwise perfect lattice sites, if the lattice is sufficiently flexible and capable of screening the local hole. One important observation of the present study is that sp mediated polarons are not particularly well localised (only 15% of the charge localised at the Bi polaron site, see Fig. 4(h)). Resultantly, at higher concentrations we find bonding and anti-bonding bipolaronic states and strong ordering tendencies. For sp systems the opening of a gap is more akin to a "long-

range" Peierls distortion than to an essentially "local" Jahn-Teller effect. Similar features can be expected for many multivalent cations. From a computational point, our study demonstrates that hybrid functionals describe multivalent cations as well as the resultant polaronic lattice distortions outstandingly well, and represent a major and "not just quantitative" step forward in the modelling of oxides. We believe that the successful description of the insulating oxide $\text{Ba}_{1-x}\text{K}_x\text{BiO}_3$ will spur similar research in a wide class of complex physical phenomena such as trapping of electrons and holes in high- k dielectric materials or organic semiconductors, or confinement at the interface between metallic and insulating oxides.

-
- [1] Y. Tokura, N. Nagaosa, *Science* **289**, 462 (2000).
 - [2] N. F. Mott, *Rev. Mod. Phys.* **40**, 677 (1968).
 - [3] M. Imada, A. Fujimori, Y. Tokura, *Rev. Mod. Phys.* **70**, 1041 (1998).
 - [4] C. H. Ahn, J.-M. Triscone, Mannhart, J., *Nature* **424**, 1015 (2003).
 - [5] K. Ueno, *et al.*, *Nature Mat.* **7**, 855 (2008).
 - [6] R. J. Cava, *et al.*, *Nature* **347**, 814 (1988).
 - [7] J. M. Ziman, Oxford Univ. Press, Oxford, 1960.
 - [8] D. E. Cox, A. W. Sleight, *Solid State Commun.* **19**, 969 (1976).
 - [9] W. A. Harrison, *Phys. Rev. B* **74**, 245128 (2006).
 - [10] S. Pei, *et. al*, *Phys. Rev. B* **41**, 4126 (1990).
 - [11] L. F. Mattheiss, D. R. Hamann, *Phys. Rev. B* **28**, 4227 (1983).
 - [12] K. Kunc, *et al.*, *Solid State Comm.* **80**, 325 (1991).
 - [13] T. Thonhauser, K. M. Rabe, *Phys. Rev. B* **73**, 212106 (2006).
 - [14] S. Tajima, *et al.*, *Phys. Rev. B* **32**, 6302 (1985).
 - [15] R. O. Jones, O. Gunnarsson, *Rev. Mod. Phys.* **61**, 689 (1989).
 - [16] A. I. Liechtenstein, V. I. Anisimov and J. Zaanen, *Phys. Rev. B* **52**, R5467 (1995).
 - [17] A. D. Becke, *J. Chem. Phys.* **98**, 1372 (1993).
 - [18] A. V. Krukau, O. A. Vydrov, A. F. Izmaylov, G. E. Scuseria, *J. Chem. Phys.* **125**, 224106 (2006).
 - [19] G. Kresse, J. Furthmüller, *Comput. Mater. Sci.* **6**, 15 (1996).
 - [20] J. Paier, R. Hirschl, M. Marsman, G. Kresse, *J. Chem. Phys.* **122**, 234102 (2005).
 - [21] L. A. Klinkova, M. Uchida, Y. Matsui, V. I. Nikolaichik, N. V. Barkovskii, *Phys. Rev. B* **67**, 140501(R) 2003.
 - [22] M. A. Karlow, *et al.*, *Phys. Rev. B* **48**, 6499 (1993).
 - [23] T. Nishio, J. Ahmad, H. Uwe, *Phys. Rev. Lett.* **95**, 176403 (2005).
 - [24] J. Ahmad, H. Uwe, *Phys. Rev. B* **72**, 125103 (2005).
 - [25] I. B. Bischofs, P. B. Allen, V. N. Kostur, R. Bhargava, *Phys. Rev. B* **66**, 174108 (2002).
 - [26] To clarify why the sc arrangement of bipolarons is unstable, we inspected the bandstructure of the metallic cubic cell [Fig. 1(b)], and found three valence bands with maxima at Γ (empty) and strong and similar 1.5 eV downward dispersion along $\overline{\Gamma X}$ and $\overline{\Gamma L}$ (states at X and L are occupied). Although this supercell is orthorhombic, the original cubic symmetry of the perovskite unit cell

prevails to a large extent in the bandstructure. A semi-conducting state can be expected only if states at Γ couple with those at L and/or X in the 8-fold supercell. At $x = 0.125$ an fcc like arrangement fulfills this criteria, whereas at $x = 0.25$, the second bipolaron must be placed such that the Bragg reflections prevail along space diago-

nals. This can be realised only by ordering all bipolarons in stripes along the face diagonals, as indicated by small red circles in Fig. 1, whereas bipolaronic conversion of the body centred atom, circled green in Fig. 1(c), destroys the Bragg reflection along the space diagonal.